



# Shearlet-Based Adaptive Noise Reduction in T Images

M. Petrov\*(C.A.)

**Abstract:** The noise in reconstructed slices of X-ray Computed Tomography (CT) is of unknown distribution, non-stationary, oriented and difficult to distinguish from main structural information. This requires the development of special post-processing methods based on the local statistical evaluation of the noise component. This paper presents an adaptive method of reducing noise in CT images employing the shearlet domain in order to obtain such an estimate. The algorithm for statistical noise assessment takes into account the distribution of signal energy in different scales and directions. The method efficiently uses the strong targeted sensitivity of shearlet systems in order to reflect more accurately the anisotropic information in the image. Because of the complex characteristics of the noise in these images, the threshold constant is determined by means of the relative entropy change criterion. The comparative analysis, which has been conducted, shows that the proposed method achieves higher values for the Peak Signal-to-Noise Ratio (PSNR), as well as lower values for the Mean Squared Error (MSE), in comparison with the other methods considered. For the MATLAB'S Shepp Logan Phantom test image, the numerical value of this superiority is on average more than 23% for the first quantitative measure, and 37% for the second. Its efficiency, which is greater than that of the wavelet-based method, is confirmed by the results obtained – the edges have been preserved during noise reduction in real CT images.

**Keywords:** Entropy of Shannon, Shearlet Decomposition, Statistical Noise Reduction, X-Ray Computed Tomography.

## 1 Introduction

QUANTUM noise in CT is a function of the discrete X-ray photons measured by the detector. Their variable number defines it as a random variable. The noise generated during intensity measurement is complemented by electronic noise and, through reconstruction algorithms of the projection data, it is transformed into pixel noise in CT slices. Because X-rays weaken due to the density and the amount of the substance through which they pass, the noise in CT images is non-stationary and oriented, characterizing the direction of the strongest attenuation.

Radiation dose reduction in CT is necessary in order to avoid potential risks to the patient's health, but the decrease in the amount of X-rays leads to a higher noise level in the resulting image. Furthermore, reducing the patient's radiation dose limits the possibility to carry out the relevant diagnostic task on the part of a radiologist. Therefore, it is important to develop methods that reduce the noise in CT images without visibly violating the spatial resolution or changing the radiation dose, for they will be widely used in the medical practice. The existing algorithmic solutions for noise reduction in low-dose CT are divided into three main groups [1]: methods in the projection data space; methods in the image space and iterative reconstruction methods.

Low PSNR values in sonograms lead to loss of structural information. The noise reduction algorithms in the projection data space are most often based on iterative, optimization and filtering techniques, with the potential use of the statistics of the photons in the CT data and multiscale transformations [2-6]. The implementation of these methods in the image recovery system is associated with high computational

Iranian Journal of Electrical and Electronic Engineering, 2021.  
Paper first received 29 April 2019, revised 06 April 2020, and accepted 10 April 2020.

\* The author is with the Faculty of Mathematics and Informatics, St. Cyril and St. Methodius University of Veliko Turnovo, Veliko Turnovo, Bulgaria.

E-mail: [m.petrov@ts.uni-vt.bg](mailto:m.petrov@ts.uni-vt.bg).

Corresponding Author: M. Petrov.

<https://doi.org/10.22068/IJEEE.17.1.1485>

complexity.

The complex characteristics of the noise in the reconstructed slices is a challenge for the noise reduction methods in the image space [7-9]. Some of the methods that achieve significant noise reduction are those based on anisotropic diffusion. The iterative nature of this diffusion allows for improved computational efficiency. However, the so-called mosaic effects appear in denoised CT images. Another group of noise reduction methods in CT slices is based on the local statistical evaluation of the noise in the domain of some multiscale transformations.

The third group of noise reduction techniques in CT refer to iterative reconstruction. They use iterative-optimization algorithms that are implemented within the two spaces in order to obtain CT images [10, 11]. Thanks to the technological development and expanded computing capabilities of workstations, the iterative reconstruction is a preferred alternative to the conventional algorithm for back projection filtering. In recent years, a significant number of publications have emerged in this field. They show the increased research interest in addressing the radiation dose reduction problem while maintaining the diagnostic properties of the image [12, 13].

The present paper proposes an adaptive method for reducing noise in CT images by locally evaluating their noise component. This statistical assessment is performed in the domain of the shearlet transform due to the effectiveness of the presentations of these multiscale and multi-directional base systems. The method is based on signal energy distribution in different scales and directions. Considering the undefined character of noise distribution in tomographic images, the adaptive threshold constant is determined by means of the entropy change criterion.

The rest of the paper is organized as follows: Section 2 provides a brief description of the theories used. Section 3 presents the proposed algorithm for noise reduction in CT images. Section 4 describes how the threshold mask is determined. The effectiveness of the method, with respect to other methods, is evaluated in Section 5, and the last part summarizes the results obtained, as well as the conclusions drawn.

## 2 Related Theories

### 2.1 The Wavelet Shrinkage Denoising Method

Most of the proposed noise reduction algorithms use a certain statistical distribution of the random variables in CT slices that may not present the actual characteristics of the noise in these images as accurately as needed. In order to solve these problems, [14, 15] propose methods for reducing noise by means of the wavelet threshold method based on the correlation between two CT images that are equivalent in terms of the information they contain. The idea is that, unlike structural information, the noise between the two images is

uncorrelated. Therefore, the high-correlation wavelet coefficients are maintained, whereas the low-correlation ones are suppressed.

The Adaptive Wavelet Shrinkage (AWSHrink) method for noise reduction in CT images announced in [16] has been considered in connection with the method proposed in this paper. It is adjusted to the noise by statistically evaluating its locally and orientationally dependent strength. The method can be briefly described by means of the following steps:

**Step 1:** Obtaining a pair of input images, Single-Source CT (SSCT) images or Dual-Source CT (DSCT) images. The resulting images contain identical structural information, but different noise;

**Step 2:** Wavelet decomposition of the input images;

**Step 3:** Noise evaluation of the input images through high-frequency wavelet coefficients;

**Step 4:** Averaging and thresholding;

**Step 5:** Obtaining a noise-estimated image through the inverse wavelet transformation.

### 2.2 The Shearlet Transform

Among other multiscale transformations, the Shearlet Transform (ST) is the most effective because it presents multidimensional data. Shearlet systems are introduced employing special operators: scaling operator  $D_{A_a}$  (generating elements in different scales), shearing operator  $D_{S_s}$  (ensuring orientation), and translation operator  $T_\tau$  (ensuring location). Operator  $D_{A_a}$ , ( $a \in \mathbb{R}^+$ ) is most often determined by the matrix of parabolic scaling (or dilation)  $A_a = \text{diag}(a, \sqrt{a})$ , i.e. the selected anisotropy parameter value is 0.5, whereas  $D_{S_s}$ , ( $s \in \mathbb{R}$ )

is determined through the shear matrix  $S_s = \begin{pmatrix} 1 & s \\ 0 & 1 \end{pmatrix}$

and  $T_\tau \phi(t) = \phi(t - \tau)$ . The continuous shearlet system for the function  $\psi \in L_2(\mathbb{R}^2)$  and the ST of the function  $f \in L_2(\mathbb{R}^2)$  associated with it are defined by means of (1) and (2), respectively [17]:

$$\begin{aligned} \{\psi_{a,s,\tau}(t) &= T_\tau D_{S_s} D_{A_a} \psi(t) \\ &= a^{-3/4} \psi(A_a^{-1} S_s^{-1}(t - \tau)); a \in \mathbb{R}^+, s \in \mathbb{R}, \\ &\tau \in \mathbb{R}^2\}, \end{aligned} \quad (1)$$

$$ST_{\psi} f(a, s, \tau) = \langle f, \psi_{a,s,\tau} \rangle = \int_{\mathbb{R}^2} f(t) \cdot \overline{\psi_{a,s,\tau}(t)} dt, \quad (2)$$

where  $\overline{\psi_{a,s,\tau}}$  is the complex conjugate of  $\psi_{a,s,\tau}$ .

There are various algorithms for the implementation of the respective discrete shearlet transforms. The present paper uses the Fast Finite Shearlet Transform (FFST) algorithm proposed by S. Häuser and implemented on the basis of cone-adapted continuous

shearlet systems [18]. Meyer’s function is used for the construction of the classical shearlet, and the proposed algorithm is based on fast discrete Fourier transforms. The resulting discrete shearlet system  $\{\psi_{j,k,m}^\kappa(\omega)\}$  forms a Parseval frame of the finite Euclidean space, a subspace of  $L_2(\mathbb{R}^2)$ , which provides the construction of the Inverse Discrete Shearlet Transform (IDST).

### 3 The Proposed Method

#### 3.1 An Introduction to the Method

The method described in Section 2.1 has resulted from the need of a compromise between noise reduction in the regions containing edges and edge preservation in the CT image. In connection with this method, the algorithm of noise reduction in CT images developed in this paper uses the shearlet domain in order to obtain the local statistical noise assessment and the quantitative criterion for determining the threshold constant based on Shannon entropy. The proposed method for reducing the noise in CT images by means of FFST can be represented by the diagram in Fig.1.

If a DSCT scanner is not available, the required two input images can be obtained by means of a SSCT scanner, acquiring two consecutive scans of the subject under identical circumstances. In order to avoid exposing the patient to radiation twice, these images can be obtained in one scan, by two separate reconstructions of two non-intersecting subsets of the complete set of projection data. Furthermore, for each of the two sets of projection data, the conditions of the sampling theorem must be met. In addition, the averaged image of the two reconstructions obtained corresponds to the image reconstructed from the full set of projections [19].

#### 3.2 Noise Assessment

Let  $I_1$  and  $I_2$  be the input CT images obtained by a separate reconstruction from the even and odd numbered projections, assuming that the number of the full set of projection data is an even number.

If  $I_0$  indicates the general structural information, and  $N_1$  and  $N_2$ , ( $N_1 \neq N_2$ ) denote the respective additive noise components having zero average values, then these images are represented by the following equation:

$$I_i = I_0 + N_i, (i = 1, 2). \tag{3}$$

The division of the projection data implies that the

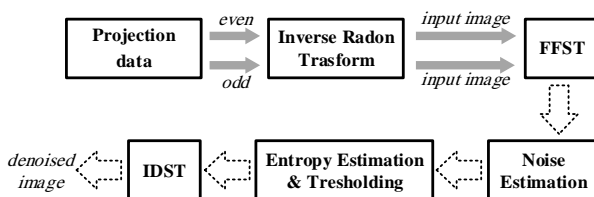


Fig. 1 A block diagram of the proposed method for reducing noise in CT images.

number of the quanta that produce them is approximately equal. Therefore, it can be assumed that the standard deviation of the noise in the two images is the same for each pair of corresponding pixels, i.e.  $\sigma(I_1) \approx \sigma(I_2)$ . Furthermore, the noise level in each of the images is increased by a factor of  $\sqrt{2}$  compared to the noise level in the reconstructed slice of the full set of projections [19]. Using (3), the standard deviation of the noise in the input images can be calculated by the following equation

$$D = I_1 - I_2 = N_1 - N_2. \tag{4}$$

Let  $c_{j,k,m}^\kappa(I_i) = \langle I_i, \psi_{j,k,m}^\kappa \rangle$ , ( $i = 1, 2; \kappa \in \{0, h, v, h \times v\}$ ) (See [18]) be the shearlet coefficients of the two images. Then, according to (4), the coefficients of the noise representations are

$$c_{j,k,m}^\kappa(D) = c_{j,k,m}^\kappa(I_1) - c_{j,k,m}^\kappa(I_2), \tag{5}$$

using the fact that FFST is a linear transformation. The noise between the two sets of projection data used is uncorrelated. Therefore, it is uncorrelated in the reconstructed images, too. By means of (4), the following estimates of the standard noise deviations in the input images are obtained

$$\sigma(I_1) = \sigma(I_2) = 2^{-0.5} \cdot \sigma(D). \tag{6}$$

Because the noise strength in CT images is spatially dependent, its standard deviation for each pixel is calculated locally within a particular neighborhood. The estimation of this local value is obtained by (5), selecting for each pixel  $m$  a neighborhood  $\Omega_m$ , which contains  $n$  pixels. Thus,

$$\sigma_{j,k,m}^\kappa(D) = \sqrt{n^{-1} \cdot \sum_{n \in \Omega_m} c_{j,k,m}^\kappa(D)^2}, \tag{7}$$

since the noise has a zero average value. The results obtained by means of (7) are used to calculate the local values of the standard deviation of the noise in the averaged image

$$\sigma_{j,k,m}^\kappa(I) = 2^{-0.5} \cdot \sigma_{j,k,m}^\kappa(I_1) = 2^{-1} \cdot \sigma_{j,k,m}^\kappa(D), \tag{8}$$

where  $I = 0.5(I_1 + I_2)$  and the second equality is based on (6). By means of (8), the threshold value adapted to the shearlet parameters is defined as:

$$\eta_{j,k,m}^\kappa(r) = 2^{-1} \cdot r \cdot \sigma_{j,k,m}^\kappa(D) \tag{9}$$

Therefore, the amount of the suppressed noise is regulated by the threshold parameter  $r$ .

#### 3.3 Determining the Threshold

In information theory, entropy is regarded as the

quantitative measure of the information that we are interested in. For the purpose of the task under consideration, the noise level in the image in question is considered information [20]. Shannon entropy is used as a quantitative criterion for determining the threshold value for processing high-frequency shearlet coefficients [21]. It is set by (10)

$$E_r = -\sum_m \eta_{j,k,m}^\kappa(r) \cdot \log_2(\eta_{j,k,m}^\kappa(r))^2 \quad (10)$$

For this purpose, the change rate of this entropy is evaluated for each sub-band in the shearlet domain by its relative change:

$$\frac{dE}{E_r}(\kappa, j, k) = \frac{|E_{r+1} - E_r|}{|E_r|} \quad (11)$$

along a provisional graded scale for parameter  $r$ . Thus, the established value of parameter  $r$ , which is assumed to be optimal, sets the final threshold value  $\eta_{j,k,m}^\kappa(r_0)$  (See (9)) for processing the coefficients from the corresponding sub-band. The way of determining parameter  $r_0$  for a certain image and a fixed sub-band of the shearlet domain is presented in Section 4.

### 3.4 Obtaining the Noise Estimated Image

There are different threshold processing rules in shrinkage methods when reducing noise in the obtained data. The most popular ones are the nonlinear functions of the “hard” and “soft” thresholds introduced by Donoho and Johnstone [22]. The algorithm of the proposed estimation includes: decomposition of the noisy signal by means of a wavelet transform; evaluation of the established wavelet coefficients by means of a selected threshold value and obtaining the estimated signal through the inverse wavelet transform. The main idea is that only a small number of wavelet coefficients bear the structural information of the image. Image denoising is based on shrinking wavelet coefficients towards zero. Due to the discontinuity of the function, small changes in the processed data become a problem for hard threshold processing. The proposed algorithm employs the continuous function of the soft threshold, and the evaluated high-frequency shearlet coefficients of the image  $I$  are:

$$\tilde{c}_{j,k,m}^\kappa(I) = \text{sgn}(c_{j,k,m}^\kappa(I)) \cdot \max(|c_{j,k,m}^\kappa(I)| - \eta_{j,k,m}^\kappa(r_0), 0), \quad \kappa \neq 0 \quad (12)$$

At the end, the method for obtaining the estimated image makes use of the application of IDST for the array consisting of the coefficients defined by (12) and the unchanged coefficients from the low-frequency domain  $-c_{j,k,m}^0(I)$ . The resulting CT image is expected to have an improved signal-to-noise ratio and

an increased diagnostic value, i.e. to keep the anatomical structures.

### 4 Experimental Determination of the Optimum Threshold Parameter

High-frequency wavelet coefficients carry information not only on the local peculiarities of the image, but also on its noise component, as specified in Section 3.2. There are some risks when determining the threshold noise constant for processing these coefficients in the wavelet shrinkage methods. The results obtained by the wavelet shrinkage methods are directly related to the threshold values. The main threshold values proposed in [22] as arguments for the hard and soft threshold functions are the universal and minimax thresholds. The disadvantage of the theoretical models developed to evaluate or reconstruct a given signal from its empirical results is that this data is damaged by additive white Gaussian noise.

The unknown character of the distribution of the noise component in CT images requires another approach to this task. The final determination of the threshold constant, according to the proposed method, is based on the relative entropy change (See (11)) regarding the eight-graded scale of weight coefficient  $r$  and (9). Fig. 2 shows the results of the determination of threshold constant  $\tau_{0,0,m}^h(r)$  for the Cardiac, Spine and Head test images (See Section 5.2). The resulting graphs shows that, for each of the three images, the entropy change rate is low up to the fourth level, which means that their noise information has been gradually reduced. However, after the fourth level, this speed sharply increases, which means that the nature of the information surveyed has changed. Based on this observation, it can be concluded that, after the fourth level, local image peculiarities are levelled off. Therefore, as an optimal threshold parameter value, we can accept  $r_0 = 4$  for each of the three images in the shearlet sub-band:  $\kappa = h, j = k = 0$ . The greater values of this parameter lead to zero shearlet coefficients having predominantly structural image information. By means of the obtained threshold

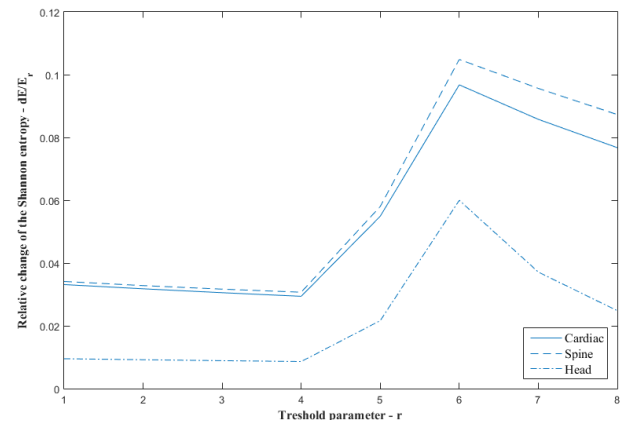


Fig. 2 Graphs showing the dependency of the relative entropy change on the threshold parameter values (for Cardiac, Spine and Head CT images; shearlet sub-band:  $\kappa = h, j = k = 0$ ).

$\tau_{0,0,m}^h (r_0 = 4)$ , a soft threshold processing of the high-frequency coefficients of the averaged image  $I$  is carried out in the corresponding shearlet sub-band.

**5 Results and Comparative Analysis**

The effectiveness of the proposed method for reducing noise in CT images is assessed using two types of data, phantom and real tomographic images. The main objectives of the experiments carried out in the comparative analysis are related to the issues of noise suppression and structure preservation. Since this method is oriented to the sub-bands in the shearlet domain, the comparison is performed by means of shearlet-adapted methods using some known threshold constants that depend on the decomposition level:

- Adapted BayesShrink (ABSrink) algorithm [23]

$$-T_{j,k}^B = \frac{\sigma_{j,k}^2}{\sigma_{j,k,m}}$$

where  $\sigma_{j,k}$  is the standard deviation

of the noise in the sub-band having scale  $j$  and direction  $k$ , and  $\sigma_{j,k,m}$  is the standard deviation of the  $m$ -th coefficient in that part of the shearlet domain.

- Adapted VisuShrink (AVShrink) algorithm [24]

$$-T_{j,k}^V = \sqrt{2 \cdot \log_2 N} \cdot 2^{(j-J)/2} \cdot \text{Median}(|w_{j,k,m}|_m) / .6745,$$

where  $w_{j,k,m}$  is the corresponding shearlet coefficient and  $j = j_0, \dots, J$ .

The soft threshold function, which gives better results than the hard threshold, due to its continuity, is used to implement these two algorithms. Wavelet shrinkage methods can be preceded by processing the detailed coefficients by means of a sigmoid function in order to improve the quality of the medical images obtained at a reduced radiation dose [25]. In the comparative analysis, the sigmoid function represented by (13)

$$\text{sigm}(x) = (1 + e^{-x})^{-1}, \tag{13}$$

is additionally applied to the AVShrink algorithm, and the resulting combined method is called SIGMOID.

Two of the quantitative measures used to evaluate these noise reduction methods in CT images are MSE and PSNR. The values of these two functions are easily calculated on the basis of the intensity of the distortions, but they are not reliable measures for visual accuracy. The Structural Similarity Index (SSIM) is used as quantitative assessment of the visual similarity of the original image and its noise approximation.

**5.1 Phantom Data**

The test image in the first comparative analysis experiment is an improved contrast version of the Sheep-Logan Phantom – MATLAB’s Shepp Logan Phantom. Since the universal threshold in noise suppression methods is intended for white Gaussian noise, a computer-generated Additive White Gaussian Noise (AWGN) having different values of the standard deviation  $\sigma$  is added to the image.

Table 1 provides the experimentally obtained results for the quantitative measures PSNR and MSE for each of the four noise reduction methods in the image, for  $\sigma = 0.1; 0.15; 0.2; 0.25; 0.3$ , respectively.

The data in this table shows that the proposed method achieves higher values for PSNR and lower values for MSE for all AWGN levels. This superiority is presented numerically as follows: PSNR – on average 24.6%, and MSE – on average 37.3%, for all levels of AWGN.

Fig. 3 presents the comparative graphs illustrating the variation of SSIM values according to standard noise deviation  $\sigma$  in the methods used in the comparative analysis. Obviously, the proposed method achieves better values for this index than the other three methods. Moreover, in the visual quality assessment, it is observed that this method is less sensitive to the noise level. Therefore, this experimental data shows that our method is superior to the other methods discussed so far according to all three metric functions.

**5.2 Real CT Data**

The second experiment, part of the comparative

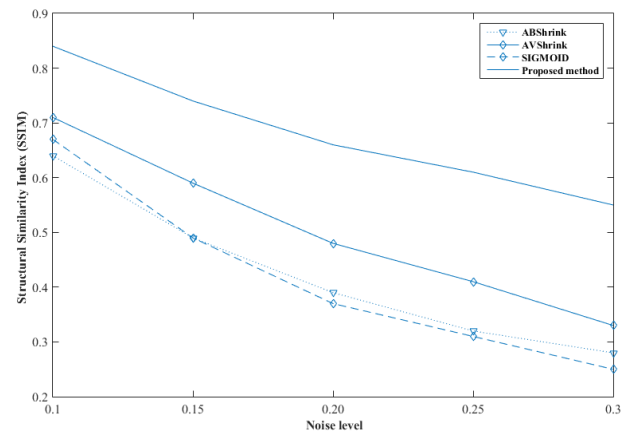


**Fig. 3** Graphs of the dependency of the SSIM on the noise level for the different methods.

**Table 1** Quality measure values for the different noise reduction methods.

$\sigma$	ABSrink		AVShrink		SIGMOID		Proposed method	
	PSNR	MSE	PSNR	MSE	PSNR	MSE	PSNR	MSE
0.10	32.13	39.78	36.68	88.36	35.88	29.96	42.45	19.21
0.15	30.07	63.93	33.88	134.05	31.90	61.46	39.05	28.27
0.20	27.31	120.74	31.55	172.87	29.19	96.84	36.57	42.55
0.25	26.17	156.83	29.81	183.86	27.26	138.07	34.61	52.74
0.30	24.44	233.56	28.22	244.73	25.58	198.34	32.88	53.99

analysis performed to evaluate the effectiveness of the noise reduction methods in CT images, uses Cardiac, Spine and Head medical images. They are in DICOM output format and were taken by the Siemens - Somatom Definition and Somatom Spirit CT scanners at St. Marina Hospital, EAD in Varna, Bulgaria.

Figs. 4, 5, and 6 show both the actual images and their corresponding noise-estimated images, as well as the residual information that has been removed from the image when applying these two algorithms, in order to compare the visual effect after AWSHrink and the proposed method for reducing the noise in these tomographic images.

The residual information obtained by means of the reduction methods is perceived as noise removed from the original image. Unlike AWSHrink, the proposed method maintains more structural details in each of the three tested images. This is illustrated by Figs. 4(b), 4(c), 5(b), 5(c), 6(b), and 6(c), which show the differences between the original and evaluated images. In fact, the second (b) images contain a greater number of small details than the second (c) images. Similar results are obtained with other test images. Therefore, the shearlet-based method achieves better edge preservation and more effective noise reduction in CT images.

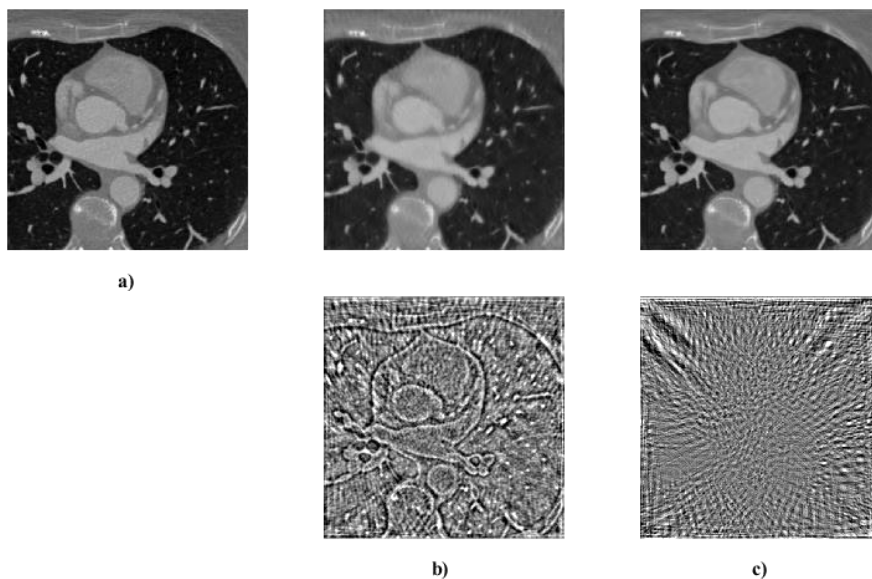


**Fig. 4** Results of the reduction of noise in CARDIAC image by means of different methods: a) Original image, b) Denoised image and the corresponding residual information, obtained through AWSHrink, and c) Denoised image and the corresponding residual information, obtained through the proposed method.

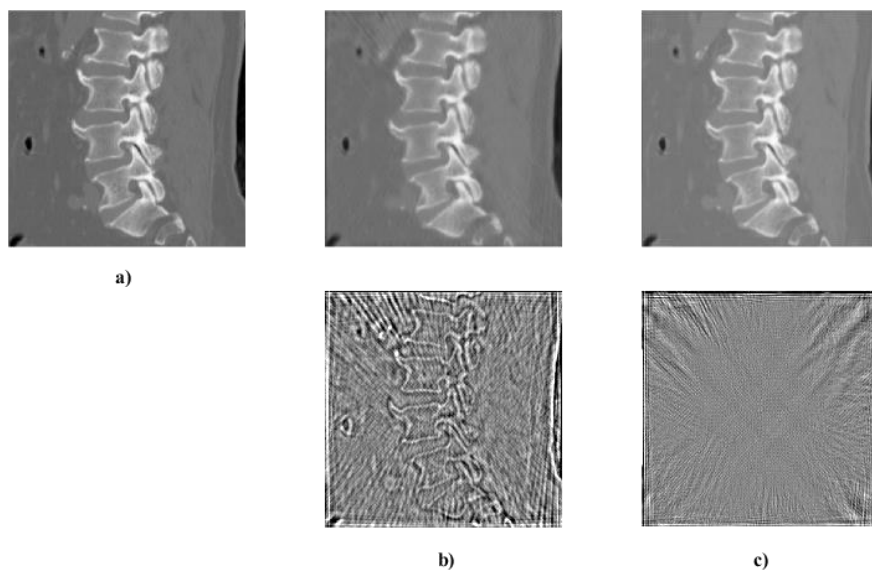


**Fig. 5** Results of the reduction of noise in SPINE image by means of different methods: a) Original image, b) Denoised image and the corresponding residual information, obtained through AWSHrink, and c) Denoised image and the corresponding residual information, obtained through the proposed method.

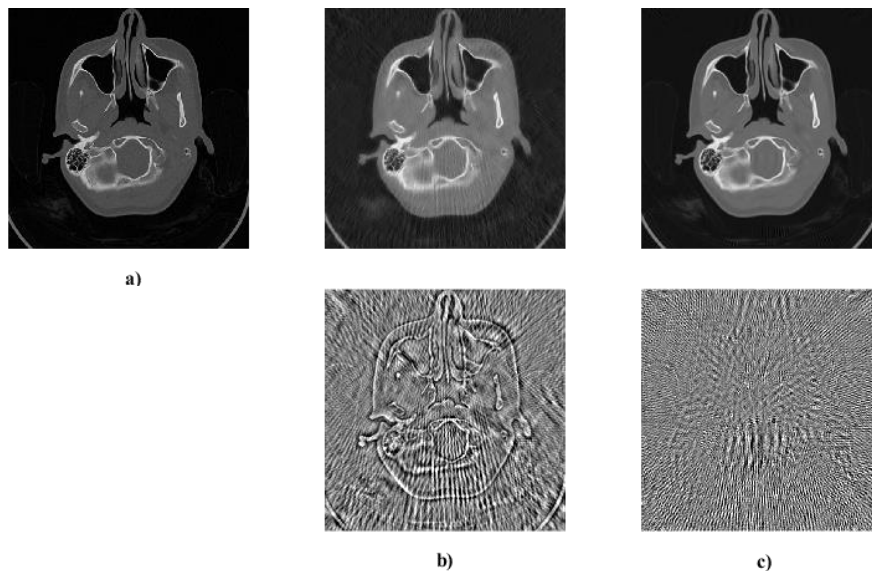


**Fig. 6** Results of the reduction of noise in HEAD image by means of different methods: a) Original image, b) Denoised image and the corresponding residual information, obtained through AWSHrink, and c) Denoised image and the corresponding residual information, obtained through the proposed method.

## 6 Conclusion

Based on indirect statistical estimation in the shearlet domain, an adaptive threshold algorithm is proposed in order to reduce the noise in CT images. The proposed method uses some advantages of shearlet systems in the multiscale transformations class. The sparseness of shearlet representations is essential for shrinkage methods in the task of reducing image noise. On the other hand, through the multiscale and multi-directional characteristics of these systems, a better assessment of the noise in CT images is achieved, as compared to other multiscale methods. The choice of the threshold mask for processing the high-frequency coefficients of the averaged image is based on Shannon entropy.

In the experiments with MATLAB's Shepp Logan Phantom, the proposed method shows better results in all three quantitative measures used to assess the qualities of the noise reduction methods considered. The second group of experiments with real tomographic images also confirm the effectiveness of shrinkage methods in the shearlet domain.

The assessment of the noise in the projection data and in the corresponding reconstructed slice, as well as its reduction, is among the important tasks in the area of diagnostic X-ray CT. Its solution can become part of the strategy whose aim is to minimize the radiation risk for the patient and to improve the quality of the diagnostic image. The proposed adaptive shearlet shrinkage method is applicable during the subsequent processing of the reconstructed projection data.

## References

- [1] E. C. Ehman, L. Yu, A. Manduca, A. K. Hara, M. M. Shiung, D. Jondal, D. S. Lake, R. G. Paden, D. J. Blezek, M. R. Bruesewitz, C. H. McCollough, D. M. Hough, J. G. Fletcher, "Methods for clinical evaluation of noise reduction techniques in abdominopelvic CT," *RadioGraphics*, Vol. 34, No. 4, pp. 849–862, 2014.
- [2] P. J. La Rivière, J. Bian, and Ph. A. Vargas, "Penalized-likelihood sinogram restoration for computed tomography," *IEEE transactions on medical imaging*, Vol. 25, No. 8, pp. 1022–1036, 2011.
- [3] A. Manduca, L. Yu, J. D. Trzasko, N. Khaylova, J. M. Kofler, C. M. Mc Collough, and J. G. Fletcher, "Projection space denoising with bilateral filtering and CT noise modeling for dose reduction in CT," *Medical Physics*, Vol. 36, No. 11, pp.4911–4919, 2009.
- [4] A. Maier, L. Wigstrom, H. G. Hofmann, J. Hornegger, L. Zhu, N. Strobel, and R. Fahrig, "Three-dimensional anisotropic adaptive filtering of projection data for noise reduction in cone beam CT," *Medical Physics*, Vol. 38, No. 11, pp. 5896–5909, 2011.
- [5] S. Tang and X. Tang, "Statistical CT noise reduction with multiscale decomposition and penalized weighted least squares in the projection domain," *Medical Physics*, Vol. 39, No. 9, 5498–5512, 2012.
- [6] X. Cui, Zh. Gui, Q. Zhang, Y. Liu, and R. Ma, "The statistical sinogram smoothing via adaptive-weighted total variation regularization for low-dose X-ray CT," *Optik - International Journal for Light and Electron Optics*, Vol. 125, No. 18, pp. 5352–5356, 2014.
- [7] Z. Yang, M. D. Silver, and Y. Noshi, "Adaptive weighted anisotropic diffusion for computed tomography denoising," in *11<sup>th</sup> International Meeting on Fully Three-dimensional Image Reconstruction in Radiology and Nuclear Medicine*, Potsdam, Germany, pp. 210–213, 2011.

- [8] A. Borsdorf, "Adaptive filtering for noise reduction in X-ray computed tomography," *Ph.D dissertation*, Department of Computer Science 5, University of Erlangen, 2009. [Online]. Available on: [www5.informatik.uni-erlangen.de/Forschung/Publikationen/2009/Borsdorf09-AFF.pdf](http://www5.informatik.uni-erlangen.de/Forschung/Publikationen/2009/Borsdorf09-AFF.pdf).
- [9] M. Kumar and M. Diwakar, "CT image denoising using locally adaptive shrinkage rule in tetrolet domain," *Journal of King Saud University – Computer and Information Sciences*, Vol. 30, No. 1, pp. 41–50, 2018.
- [10] M. Beister, D. Kolditz, and W. A. Kalender, "Iterative reconstruction methods in X-ray CT," *Physica Medica*, Vol. 28, No. 2, pp. 94–108, 2012.
- [11] Y. Wang, S. Fu, W. Li, and C. Zhang, "An adaptive nonlocal filtering for low-dose CT in both image and projection domains," *Journal of Computational Design and Engineering*, Vol. 2, No. 2, pp. 113–118, 2015.
- [12] D. Qiu and E. Seeram, "Does iterative reconstruction improve image quality and reduce dose in computed tomography?," *Radiology: Open Journal*, Vol. 1, No. 2, pp. 42–54, 2016.
- [13] G. Van Eyndhoven, and J. Sijbers, *Iterative reconstruction methods in X-ray CT – Handbook of X-ray Imaging: Physics and Technology*. Boca Raton, FL, USA: CRC Press, Chapter 34, pp. 693–712, 2018.
- [14] O. Tischenko, C. Hoeschen, and E. Buhr, "An artefact-free structure-saving noise reduction using the correlation between two images for threshold determination in the wavelet domain," in *Medical Imaging 2005: Image Processing*, Vol. 5747, pp. 1066–1075, 2005.
- [15] A. Borsdorf, R. Raupach, T. Flohr, and J. Hornegger, "Wavelet based noise reduction in CT-Images using correlation analysis," *IEEE Transactions on Medical Imaging*, Vol. 27, No. 12, pp. 1685–1703, 2008.
- [16] A. Borsdorf, R. Raupach, and J. Hornegger, "Multiple CT-reconstructions for locally adaptive anisotropic wavelet denoising," *International Journal of Computer Assisted Radiology and Surgery*, Vol. 2, No. 5, pp. 255–264, 2008.
- [17] G. Kutyniok, W.Q. Lim, and G. Steidl, "Shearlets: theory and applications," *GAMM-Mitteilungen*, Vol. 37, No. 2, pp. 259–280, 2014.
- [18] S. Hauser and G. Steidl, "Fast finite shearlet transform: A tutorial," *arXiv preprint arXiv:1202.1773*, 2014.
- [19] F. Natterer, *The mathematics of computerized tomography*. Stuttgart:Wiley and B.G. Teubner, 1986.
- [20] S. Babichev, N. Babenko, O. Didyk, V. Lytvynenko, and A. Fefelov, "Chromatogram filtering using wavelet analysis with use of the criterion of entropy," *System Technology*, Vol. 6, No. 71, pp. 17–32, 2010. (in Russian).
- [21] M. Petrov, "A medical image denoising method using subband adaptive thresholding based on a shearlet transform," *Serdica Journal of Computing*, Vol. 10, No 3–4, pp. 219–230, 2016.
- [22] D. L. Donoho and I. M. Johnstone, "Ideal spatial adaptation by wavelet shrinkage," *Biometrika*, Vol. 81, No. 3, pp. 425–455, 1994.
- [23] G. Easley, D. Labate, and W. Lim, "Sparse directional image representations using the discrete Shearlet transform," *Applied and Computational Harmonic Analysis*, Vol. 25, No. 1, pp. 25–46, 2008.
- [24] D. L. Donoho, "Nonlinear wavelet methods for recovery of signals, densities and spectra from indirect and noisy data," in *Proceedings of Symposia in Applied Mathematics*, 1993.
- [25] H. Watanabe, D. Tsai, Y. Lee, and E. Matsuyama, "Dose reduction by the use of a wavelet-based denoising method Digital Radiography," *Health*, Vol. 7, No. 2, pp. 220–230, 2015.



**M. Petrov** is an assistant professor at the Department of Computer Systems and Technologies at the St. Cyril and St. Methodius University of Veliko Turnovo (Republic of Bulgaria). He received BS and MS degrees in Communications and Security Technologies and Systems. He was awarded his PhD degree - "Automated systems for Information Processing and Management" from Technical University – Sofia (Republic of Bulgaria), in 2014. His current research interests include Computer Vision, Image Processing, Communication and Computer Systems.



© 2021 by the authors. Licensee IUST, Tehran, Iran. This article is an open access article distributed under the terms and conditions of the Creative Commons Attribution-NonCommercial 4.0 International (CC BY-NC 4.0) license (<https://creativecommons.org/licenses/by-nc/4.0/>).